PIECEWISE LINEAR CYLINDER MODELS FOR 3-DIMENSIONAL AXON SEGMENTATION IN BRAINBOW IMAGERY

Erhan Bas, Deniz Erdogmus

Cognitive Systems Laboratory, ECE Department, Northeastern University, Boston, MA 02115, USA

ABSTRACT

Generalized cylinder shapes are ubiquitous in biological systems and image processing techniques to identifies these tubular objects in 3D from biomedical imagery in various modalities is a general problem of interest. One such structure that exhibits branching tubular forms are neuronal networks; specifically, recent developments in microscopy imaging technology allow researchers to acquire massive amounts of 3D color images of neural structures that need to be tracked in 3D to extract structure for the purpose of studying function. In this paper, we propose a piecewise linear generalized cylinder tracing algorithm that exploits both edge and color information in order to automatically trace axons of neurons in Brainbow imagery. Results indicate that the proposed method can successfully trace multiple axons in dense neighborhoods.

Index Terms— Locally linear generalized cylinders, axon segmentation, Brainbow

1. INTRODUCTION

Generalized cylinder shaped objects are ubiquitous in 3D biomedical imagery; many structures exhibit tree topologies with cylindrical branches (e.g., vascular networks, dendritic trees, bronchia). Consequently, significant research effort has been dedicated to the segmentation of objects with such structures that arise in various contexts [1, 2, 3]. Shape models informed by knowledge of the geometry and physical constraints of the biological structures are useful in improving automatic segmentation results; however, accurate shape models require the availability of manually segmented training data, which requires immense manual labor and time commitment to acquire. Consequently, the design of segmentation algorithms that can both aid the process of training data extraction and that can then utilize the new available data to its advantage by incorporating the information as shape priors will facilitate the development of accurate automatic segmentation approaches in this domain.

In general, since clustering based approaches are not suitable for the straightforward incorporation of shape priors, active contour and level set techniques that are based on the evolution of curves or surfaces that optimize some suitable energy function that combines multiple optimality measures, one of which imposes the desired shape prior in penalty form [4, 2], through scalarization (e.g., linear combination) are preferred. The designed energy function is used to highlight object boundaries [5] and these curve and surface evolution methods have been shown to work well in a variety of scenarios with careful tuning. These approaches, however, require a detailed level of topological and structural understanding of the dataset in order to define energy functions that will succeed. These measures are functions of image intensity (e.g., gradient-norm or other edginess metric) and spatial and shape penalties. In order to highlight certain curvilinear structures, shape filters have also been employed [6, 7]. Eigenanalysis of the Hessian matrix of the image intensity is also a popular approach to identify objects (e.g., vessels), where eigenvalue ratios can be related to local curvature [8, 7]; however, determining such relationships require extensive experience and training data.

Brainbow images, a recently developed technique for acquiring 3D colored confocal microscopy imagery that depict neuronal networks in the brain, present a great opportunity for neuroscientists to study brain structure and function; however, the speed of progress is hampered by the inability to automatically extract structural information about the network from these images due to the lack of robust and reliable 3D cylindrical object segmentation techniques for color images that could automatically trace axons (techniques designed for MR and CT specialize on intensity and they primarily focus on slice-based segmentation [1, 2, 3, 9]). Currently, researchers using Brainbow technology are limited to manual segmentation of images and tracing of axons to identify neural networks; this process is clearly cumbersome and prevents the study of large brain sections.

In this paper, we propose an algorithm for semiautomatic segmentation of objects with generalized cylinder shapes (axons) utilizing both edge and color information without making strict shape assumptions (such as curvature bounds or priors). The approach involves building piecewise linear cylinder approximations starting from a single seed point inside the axon given by the user. Future improvements will include automatic seed point identification and incorporation of information obtained from semiautomatically segmented imagery as priors. The algorithm will enable neuroscientists who acquire Brainbow images to extract 3D network structure with minimal labor and intervention.

2. BRAINBOW IMAGES & PROBLEM STATEMENT

The brain processes and propagates information through thousands of structural connections within neural networks. Understanding the organization of these 'circuits' is thought to be necessary to understand how such networks execute and adapt complex behaviors. Investigations of networks have

DE (erdogmus@ece.neu.edu) and EB (bas@ece.neu.edu) acknowledge support from NSF grants ECCS-0929576 and ECCS-0934506. The authors would also like to thank Bill Bosl and Dana Brooks for valuable discussions and to Ryan Draft for providing the Brainbow data and helping with the contents of Section 2.

been prevented, however, due to the length of 3D projections of single neurons (mm's) and the density and thinness of structures ($<$0.5 μm in diameter). The large-scale makes high-resolution imaging (serial electron microscopy) infeasible and the high density of thin structures makes resolution by diffraction-limited light microscopy impossible. To improve resolution of optical techniques, researchers have developed a genetic tool that randomly labels different neurons in mice with different colors, called 'Brainbow'. The color label is generated by random, combinatorial expression of three spectrally distinct fluorescent proteins (red, blue and green). The ratio of these proteins produces a multicolor label throughout the processes of each neuron. Neural tissues from these mice can be optically sectioned with multi-color laser-scanning confocal microscopy to render an image stack with both spectral (color) and spatial (x,y,z) resolution. To study the connections of these neurons, the resulting data set must be reconstructed manually, a process which takes months to complete, even in the simplest circuits. Thus, reconstructions have been greatly limited in quantity and complexity.

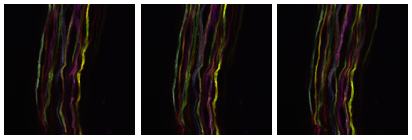

(a) $7^{th} Slice$ (b) $8^{th} Slice$ (c) $9^{th} Slice$

Fig. 1. Axial (xy-plane) slices of a sample brainbow image stack showing a bundle of axons of motor neurons connecting from the spinal cord to a muscle.

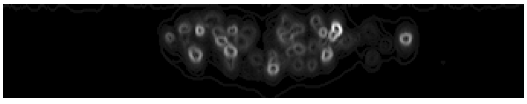

Fig. 2. Square root of the edge values in an xz-plane crossection showing circular axon boundaries.

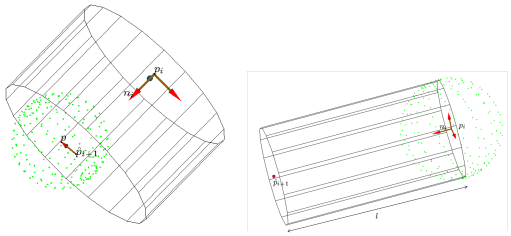

(a) Tuning Step (b) Propagation Step

Fig. 3. Tuning and propagation steps are illustrated: tuning consists of finding a sphere with center p_0 and radius r_0, as well as finding the axon propagation direction $\overline{n}$, which specifies a circular base for the local cylinder; propagation identifies the length l of the piecewise cylinder such that the surface of the cylinder follows the strong edges and the interior has a consistent color.

3. PROPOSED METHOD

Our approach uses the edge information calculated from smoothed color images to define axon boundaries. We also use the color information of fibers in our calculations to separate closely passing axons and calculating the direction of the generalized cylinder models. For a given seed voxel, the algorithm highlights each axon through a two-step process. The first step (tuning) calculates the local orientation and the corresponding perpendicular circular crossection of the axon, and the second step (propagation) identifies a cylinder with the given circular base and orientation that approximates the curved axon in a piecewise linear fashion. The process is iteratively repeated to identify a generalized piecewise linear cylinder model of the axon starting from the initial seed.

3.1. Fiber Boundary

The 3D image stack is processed jointly after resampling of each image plane to achieve cubical voxels. Preprocessing includes smoothing of the image volume using 3D bilateral filtering [10] and calculation of the edginess value for each voxel using the largest singular value of the color Jacobian with respect to voxel coordinates following an earlier similar idea utilized successfully for 2D image edge extraction [11]. It has been shown in this early work that using color gradient as a vector field will result in more robust edge detection compared to other conventional methods; furthermore, the proposed edginess measure for color images reduces to gradient norm for grayscale images. The (RGB) color Jacobian with respect to position (xyz where z is depth across image slices obtained via confocal microscopy) is

$$\mathbf{J} = \begin{bmatrix} \frac{dR}{dx} & \frac{dR}{dy} & \frac{dR}{dz} \\ \frac{dG}{dx} & \frac{dG}{dy} & \frac{dG}{dz} \\ \frac{dB}{dx} & \frac{dB}{dy} & \frac{dB}{dz} \end{bmatrix} \quad (1)$$

The largest singular value is obtained by identifying the largest eigenvalue of $\mathbf{J}^T\mathbf{J}$ as the edginess value of a voxel. The calculated edge map, $\mathbf{E}$, is used for tuning and propagation. An xz-plane crossection of the square root of the 3D edge map $\mathbf{E}$ is shown in Fig. 2 to illustrate.

3.2. Tuning

For a given seed (initial $\hat{\mathbf{p}}_0$ input) or a calculated center estimate from cylinder i (denoted by $\mathbf{C}_i$ with initial circular surface centered at $\mathbf{p}_i$ with radius r_i and axial vector $\mathbf{n}_i$ as illustrated in Fig. 3) given by $\hat{\mathbf{p}}_{i+1} = \mathbf{p}_i + l_i\mathbf{n}_i$ after propagation, we optimally identify the center $\mathbf{p}_{i+1}$, radius r_{i+1}, and direction $\mathbf{n}_{i+1}$ of the axon via the following procedure:

Step 1: The center $\mathbf{p}_{i+1}$ and radius r_{i+1} are identified by minimizing the inverse of the total edginess values on sample points $\mathbf{s}_i$ from the surface of sphere $S(\mathbf{p}; r)$ using the active-set algorithm and subject to the constraints that (i) the center of the the new sphere lies on the plane that is defined by the last circular surface of the previous cylinder, (ii) the center of the new sphere must be within r_i distance from $\hat{\mathbf{p}}_{i+1}$, (iii) the $cos(angle)$ between the color distributions of voxels in

previous cylinder and current sphere must be greater than 0.9:

$$
\begin{aligned}
(\mathbf{p}_{i+1}, r_{i+1}) \quad = \quad & \arg\min_{\mathbf{p},r} \frac{1}{\sum_i \mathcal{E}(\mathbf{s}_i;\mathbf{p},r)} \text{ subject to} \qquad (2)\\
& \mathbf{n}_i^T(\mathbf{p}-\hat{\mathbf{p}}_{i+1}) = 0\\
& (\mathbf{I}-\mathbf{n}_i\mathbf{n}_i^T)(\mathbf{p}-\hat{\mathbf{p}}_{i+1}) < r_i\\
& \frac{G(\mathbf{m}_i - \mathbf{m}_{S(\mathbf{p},r)}; \mathbf{\Sigma}_i + \mathbf{\Sigma}_{S(\mathbf{p},r)})}{G(\mathbf{0}; 2\mathbf{\Sigma}_i) G(\mathbf{0}; 2\mathbf{\Sigma}_{S(\mathbf{p},r)})} > 0.9
\end{aligned}
$$

where, $\mathbf{s}_i$ are obtained using a 21-by-21 grid in angular coordinates with $\pi/10$ radian resolution in θ (longitude) and $\pi/20$ radian resolution in ϕ (latitude)[1], $\mathcal{E}(\mathbf{s}_i;\mathbf{p},r)$ is obtained from the edge map $\mathbf{E}$ via 3D-cubic spline interpolation, and $G(\mathbf{x},\mathbf{C}) = (2\pi)^{-n/2}\det(\mathbf{C})^{-1/2}\exp(-\frac{1}{2}\mathbf{x}^T\mathbf{C}^{-1}\mathbf{x})$, with $\mathbf{m}_i$ & $\mathbf{\Sigma}_i$ being the estimated mean and covariances of the Gaussian color distribution model in RGB space for the voxels in the last cylinder (denoted by index i), and $\mathbf{m}_{S(\mathbf{p},r)}$ & $\mathbf{\Sigma}_{S(\mathbf{p},r)}$ similarly being the estimated color mean and covariances for the voxels in the current sphere $S(\mathbf{p};r)$. The mean and covariance estimates are obtained using Expectation-Maximization (EM) with a Gaussian color density model. Note that if we define the inner product between two Gaussian densities $G_j = G(\mathbf{x}-\mathbf{m}_j;\mathbf{\Sigma}_j)$ for $j=1,2$ as $< G_1, G_2 >= \int G(\mathbf{x}-\mathbf{m}_1;\mathbf{\Sigma}_1)G(\mathbf{x}-\mathbf{m}_2;\mathbf{\Sigma}_2)d\mathbf{x}$, then

$$
\frac{< G_1, G_2 >}{(< G_1, G_1 >< G_2, G_2 >)^{1/2}} = \frac{G(\mathbf{m}_1-\mathbf{m}_2;\mathbf{\Sigma}_1+\mathbf{\Sigma}_2)}{G(\mathbf{0};2\mathbf{\Sigma}_1)G(\mathbf{0};2\mathbf{\Sigma}_2)} \qquad (3)
$$

Step 2: The direction $\mathbf{n}_{i+1}$ is identified as the largest eigenvector (whose sign is selected such that it makes a positive inner product with $\mathbf{n}_i$) of a weighted covariance matrix $\mathbf{W}$ of voxel coordinate vectors for each voxel $\mathbf{v}_j$ in a cube that contains sphere $S(\mathbf{p}_{i+1}, r_{i+1})$ and that has edges aligned with the xyz-axes of the image coordinate system. The weight of each voxel is obtained from the Gaussian color model identified from the voxels inside the sphere using EM as described in step (1). Specifically:

$$
\mathbf{W} = \sum_j G(\mathbf{d}_j; s^2\mathbf{I}) G(\mathbf{c}_j - \mathbf{m}_{S_{i+1}}; \mathbf{\Sigma}_{S_{i+1}}) \mathbf{d}_j\mathbf{d}_j^T \qquad (4)
$$

where $\mathbf{d}_j = \mathbf{v}_j - \mathbf{p}_{i+1}$ is the displacement of voxel j from the center of the current sphere $S_{i+1} = S(\mathbf{p_{i+1}}, r_{i+1})$.

3.3. Propagation

Once the circular crossection of the cylinder is identified using the tuning process described above, a linear extension of the cylinder in the direction pointed to by $\mathbf{n}_i$ is generated using increments of length equal to the edge of one cubic voxel until a criterion leaves the margin determined by adaptively set lower and upper bounds. The criterion in particular, for a given cylinder of length l, is given by:

$$
\begin{aligned}
\Upsilon(l) \quad = \quad & \sum_k \mathcal{E}(\mathbf{q}_k; C(\mathbf{p}_{i+1}, r_{i+1}, l\mathbf{n}_i))\\
& -l\sum_j \mathcal{E}(\mathbf{s}_j; B(\mathbf{p}_{i+1}, r_{i+1}, \mathbf{n}_i)) \qquad (5)
\end{aligned}
$$

where $C(\mathbf{p}_{i+1}, r_{i+1}, l\mathbf{n}_i)$ is a cylinder with base center $\mathbf{p}_{i+1}$, radius r_{i+1}, with length l in the direction of $\mathbf{n}_i$, and $\mathbf{q}_k$ are samples from its surface taken on a uniform grid along the angle of the circular base (with $\pi/10$ rad resolution) and length (at a resolution of one voxel). Similarly, $B(\mathbf{p}_{i+1}, r_{i+1}, \mathbf{n}_i)$ is the base of this cylinder and $\mathbf{s}_j$ are samples taken uniformly from its circular boundary (at $\pi/10$ rad sample period). The lower and upper thresholds are selected to be proportional to the second term in the criterion above (specifically, we have used factors of 0.98 and 1.05).

4. RESULTS

We demonstrate selected results from the proposed method on a brainbow image set composed of 31 slices (z-direction resolution of 64 μm) with each slice being 1024×1024 pixels (x & y directions at 11 μm resolution). In the preprocessing step the images are downsampled by 3 in the x & y directions and upsampled by 2 in the z direction yielding a voxel size of $33 \times 33 \times 32$ μm^3. The resampled image stack is smoothed in 3D using a bilateral filter with Gaussian kernel with diagonal covariance (spatial scale of 5 voxels and RGB-color scale of 0.2). Fig. 1 shows sample axial slices of the axons after smoothing and a coronal slice of the edge map, $\mathbf{E}$ is shown in Fig. 2. While all axons can be identified and traced successfully, in Fig. 4 only a couple of selected axons are displayed. In order to emphasize weak edges, we also used the square-root of the edge values to select and iterate additional fibers. Columns of Fig. 5 show two different yz-plane slices of the brainbow image stack where first row is the filtered image, second row shows the corresponding edge map slices, and the last row displays the selected fiber projections on the square-root of the edge map.

5. DISCUSSION AND FUTURE WORK

The automatic identification and segmentation of fiber/vessel-shaped objects in 3D imagery is a commonly encountered problem. Brainbow images in particular provide a novel tool for neuroscientists to study the structure of the nervous system in vitro via confocal microscopy. In this paper, we presented a method for identifying axons in 3D image sets using edge and color information with weak shape priors incorporated in the form of a piecewise linear generalized cylinder approximation and constraints imposed during the optimization process. The proposed approach, at this point, aims to be semiautomatic in order to reduce the requirement of manual labor and intervention, yet allow the neuroscientist to have control over the identified axon-tree solutions. This will enable the accumulation of more ground-truth information about axon network geometries in various parts of the nervous system, thus will allow us to improve the presented algorithm in the future further by incorporating prior information that can be extracted from such a database.

The algorithm exploits the knowledge that each branch of an axon is a generalized cylinder and approximates this form

[1] A better sampling strategy can be achieved by using uniformly displaced grid samples on the sphere. Approximations can be done by solving a constraint optimization problem with equally displaced grid locations constraint on the sphere manifold.

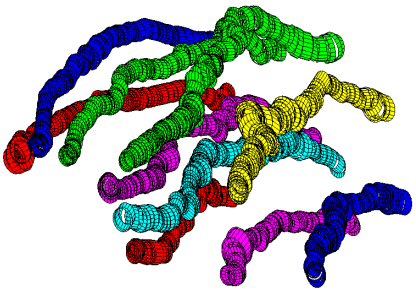

Fig. 4. Selected identified axons in a given 3D region (with axis units in voxels).

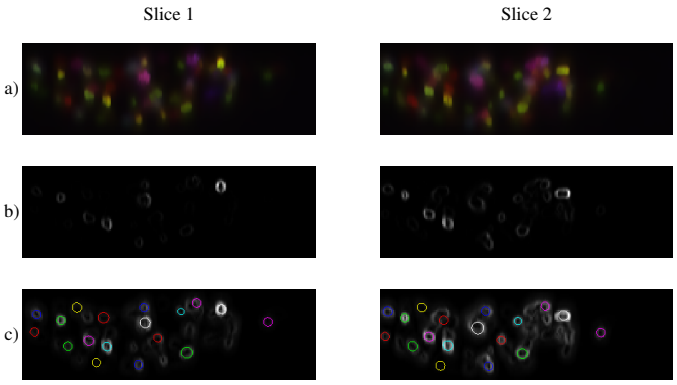

Fig. 5. a) Different Coronal (yz-plane) slices of a sample brainbow image stack b) Corresponding edge values c) Projected fibers on the image slice showing the square-root of the edge values.

using piecewise linear cylinders locally. This approach eliminates the complicated global optimization required for active shapes or level sets that minimize energy functions over the whole volume or surface. The local cylinder fitting approach results in a relatively simpler energy minimization type problem and the piecewise approximation does not lose its ability to model highly complex axon trajectories. Continuity is guaranteed by imposing constraints on the search space for consecutive cylinder pieces and the final smooth generalized cylinder can be approximated by a smooth interpolation technique such as cubic spline in 3D.

While the algorithm utilizes the edge information to fit individual local cylinders, it employs color model continuity to prevent the local cylinders from jumping from one axon to another in the vicinity. In fitting the Gaussian color density model in RGB coordinates, we used the EM algorithm instead of sample mean and sample covariance estimates for the mean and covariance. It is possible for some voxels in the given cylinder or sphere to have a multimodal color distribution (e.g. background, target axon, and a neighbor axon with a different color), thus sample statistics will be severely influenced by these additional modes, which in turn could create problems in determining the local fiber direction using the largest eigenvector of the weighted covariance matrix during the tuning step or the length of the fiber that is calculated in the propagation step. Therefore propagation purely based on the edge values is not preferred and color values of the voxels are utilized.

Problem formulation favors uniformly distributed strong edges having larger edge values which lead to easier segmentation of fibers. Depending on the location and the color, edge values vary throughout the dataset; thus proposed method assumes local thresholding strategy to adaptively select upper and lower bounds in the propagation step. Moreover, in order to emphasize the weak edges having smaller edge values, the square-root of the edge values are used. Choice of using the square-root of the edge values is heuristic and future work includes image enhancement strategies that will enable us to get more uniform edge value distributions throughout the dataset.

A desirable feature in semi-automatic segmentation is the ability of the user to intervene with the solution in a flexible and local manner. The proposed method gives the opportunity to the user to intervene in the initialization and propagation of each local cylinder while such interventions are not trivial to implement to the user's satisfaction in active shape or level set type approaches.

Since direct interventions from the user is always possible at each local cylinder, online corrections to the segmentation result are possible. Future work includes an online segmentation algorithm that adaptively calculates edge values that takes into consideration the local neighborhood. Interactive segmentation of a fiber for the selected seed point will be incorporated with the knowledge of the previously segmented fibers. This iterative and interactive segmentation approach will also enable easy segmentation of weaker fibers by segmenting the strong edges first and eliminating the effects of segmented edges by incorporating them as inequality constraints.

6. REFERENCES

[1] Wengang Zhou, Houqiang Li, and Xiaobo Zhou, "3d dendrite reconstruction and spine identification," in *Proc. of MICCAI '08, Part II*, Berlin, Heidelberg, 2008, pp. 18–26, Springer-Verlag.

[2] Delphine Nain, Anthony Yezzi, and Greg Turk, "Vessel segmentation using a shape driven flow," in *in Proc. of MICCAI'04*, 2004, pp. 51–59.

[3] Alexandra La Cruz, Matús Straka, Arnold Köchl, Milos Srámek, Meister Eduard Gröller, and Dominik Fleischmann, "Non-linear model fitting to parameterize diseased blood vessels," in *IEEE Visualization 2004*, IEEE, Ed. Institute of Computer Graphics and Algorithms, Vienna University of Technology, 2004, pp. 400–393, IEEE.

[4] Mikal Rousson, Nikos Paragios, and Rachid Deriche, "Active shape models from a level set perspective," 2003.

[5] Stanley Osher and James A. Sethian, "Fronts propagating with curvature dependent speed: Algorithms based on hamilton-jacobi formulations," *Journal of Computational Physics*, vol. 79, pp. 12–49, 1988.

[6] Yoshinobu Sato, Shin Nakajima, Hideki Atsumi, Thomas Koller, Guido Gerig, Shigeyuki Yoshida, and Ron Kikinis, "3d multi-scale line filter for segmentation and visualization of curvilinear structures in medical images," in *Proc. of CVRMed-MRCAS'97*, London, UK, 1997, pp. 213–222, Springer-Verlag.

[7] Alejandro F. Frangi, Ro F. Frangi, Wiro J. Niessen, Koen L. Vincken, and Max A. Viergever, "Multiscale vessel enhancement filtering," 1998, pp. 130–137, Springer-Verlag.

[8] Xin Gao Yisheng Zhu Stephen T.C. Wong Xiangjun Zhu, Zhong Xue, "Voles: Vascularity-oriented level set algorithm for pulmonary vessel segmentation in image guided intervention therapy," in *Proc. of ISBI'09*.

[9] R. Manniesing, B. K. Velthuis, M. S. van Leeuwen, I. C. van der Schaaf, P. J. van Laar, and W. J. Niessen, "Level set based cerebral vasculature segmentation and diameter quantification in ct angiography," *Medical Image Analysis*, vol. 10, no. 2, pp. 200–214, April 2006.

[10] C. Tomasi and R. Manduchi, "Bilateral filtering for gray and color images," 1998, pp. 839–846.

[11] H.-C. Lee and D.R. Cok, "Detecting boundaries in a vector field," *IEEE Trans. on Signal Processing*, vol. 39, no. 5, pp. 1181–1194, May 1991.